

Identification of in-vessel phenomena during severe accident using wall temperature outside of reactor vessel

Jung Taek Kim¹, Anil Kumar Khambampati², Seop Hur¹, Sung Joong Kim³ and Kyung Youn Kim^{2*}

¹Research Div. of Autonomous Control, Korea Atomic Energy Research Institute, South Korea, *jtkim@kaeri.re.kr*

²Department of Electronic Engineering, Jeju National University, South Korea

³Department of Nuclear Engineering, Hanyang University, South Korea

1. Introduction

Though a lot of analysis and research on SA has been carried out right from the development of nuclear industry, all of the possible circumstances have not been taken into consideration. Therefore, in order to further improve the efficacy of the safety of nuclear power plants, additional analytical studies that can directly monitor severe accident phenomena are needed. This paper presents an interacting multiple model (IMM) based fault detection and diagnosis (FDD) approach for identification of in-vessel phenomena in order to provide the accident propagation information using reactor vessel (RV) out-wall temperature distribution during severe accidents in nuclear power plant. The in-vessel phenomena such as core meltdown, corium relocation, reactor vessel damage, reflooding, etc. can be identified using the proposed IMM-FDD method based on the RV out-wall wall temperature distribution. The proposed IMM-FDD method is tested with five different types of SA scenarios and the results show that the temperature can be estimated with good accuracy and hence it can be used to identify the series of in-vessel phenomena.

2. Models for wall temperature evolution

Let us consider the state variables to be estimated are temperature, rate of temperature and second order rate of temperature. That is $n_x = 3$ and $x_k = [T \ dT \ dT^2]^T$ for temperature estimation. In the first model for SA identification, let us consider simple model where we estimate temperature alone $x_k = [T]$. The measurements we have are the outer wall temperature, i.e., observation matrix takes the form $H = [1 \ 0 \ 0]$. Using the random walk model described before we have the state transition matrix, measurement and noise gain matrix has the form [1, 9]

$$F = \begin{bmatrix} 1 & 0 & 0 \\ 0 & 0 & 0 \\ 0 & 0 & 0 \end{bmatrix}, T = \begin{bmatrix} 0 \\ 0 \\ 0 \end{bmatrix}, H = [1 \ 0 \ 0] \quad (1)$$

Next models, we take into account the first- and the second-order derivatives of state variable temperature. Originally the Kinematic models were developed in the target tracking field [1] to estimate the maneuvering target, in which the acceleration and the jerk are considered as white Gaussian noise for the first- and second- order kinematic models, respectively. Using Equations of motion, the motion of an

object can be represented using velocity and acceleration. Therefore, if the temperature change is linear it can be considered similar to the case where object is moving with constant velocity (CV). In CV model, the state variables are the temperature and rate of temperature $x_k = [T \ dT \ 0]^T$.

Assuming acceleration term as noise, i.e. $\ddot{x} = w_k$, the equations of motion can be written as

$$\dot{x}_{k+1} = x_k + k w_k \quad (2)$$

$$x_{k+1} = x_k + k x_k + \frac{1}{2} w_k k^2 \quad (3)$$

Using the above equations, the state transition model for constant velocity can be represented as [9]

$$F = \begin{bmatrix} 1 & k & 0 \\ 0 & 1 & 0 \\ 0 & 0 & 0 \end{bmatrix}, T = \begin{bmatrix} \frac{k^2}{2} \\ k \\ 0 \end{bmatrix}, H = [1 \ 0 \ 0],$$

here, k is time step or sampling interval (4)

And if the temperature has nonlinear behavior then it can be considered similar to the case where the object is moving with constant acceleration (CA). Here the state variables are temperature, rate of temperature and second order rate of temperature $x_k = [T \ dT \ dT^2]^T$. In this case the state transition model has the form [27]

$$F = \begin{bmatrix} 1 & k & \frac{k^2}{2} \\ 0 & 1 & k \\ 0 & 0 & 1 \end{bmatrix}, T = \begin{bmatrix} \frac{k^2}{2} \\ k \\ 1 \end{bmatrix}, H = [1 \ 0 \ 0] \quad (5)$$

3. IMM FDD scheme for identification of SA sequences

A fault detection and diagnosis (FDD) algorithm is developed using interactive multiple model scheme to identify series of events in SA scenario. The measured data input to the IMM algorithm are the temperature data (7 points) from the sensors located along outside the reactor vessel. IMM FDD algorithm for temperature starts with an initial guess for temperature, rate of temperature and second order rate of temperature and estimates the wall temperature distribution (T). The estimated rate of temperature (dT) enables us to identify the time when the temperature rises or falls is very sharp thus it can be used to identify events of SA. The IMM FDD scheme for identification of events of SAs is illustrated in flow diagram Figure 1 given below.

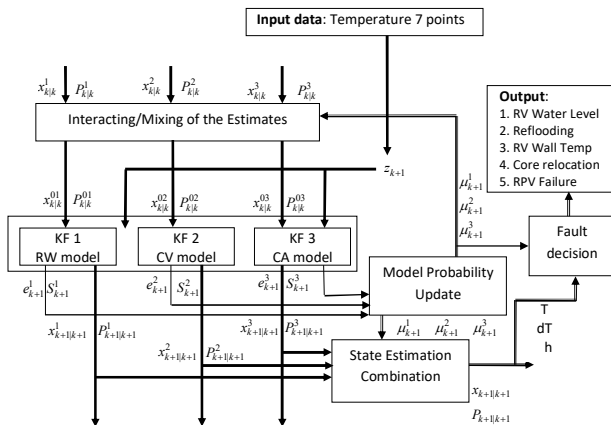


Figure 1. IMM FDD algorithm for identification of sequences of SAs using wall temperature

4. Simulation of Wall temperature distribution

The temperature distribution of inside and outside of core and on the wall, outside of reactor vessel is simulated for the validation of prediction of wall temperature. For the estimation of relationship with increasing of wall temperature in terms of increasing core temperature during sequence of SAs, the temperature distribution of core cell, core baffle, flow of core bypass, support barrel, downcomer, wall of reactor pressure vessel(RPV) cylinder and lower header are calculated using MELCOR Code, which analyzes the phenomena of severe accidents. For this simulation, design data of OPR 1000, Korean Standard Nuclear Power Plants, is used. Two high pressure accidents, such as SBO (Station Blackout), TLOFW (Total Loss of FeedWater) and 3 low pressure LOCA accidents, such as SBLOCA(Small Break Loss Of Coolant Accident), MBLOCA (Medium Break LOCA) and LBLOCA(Large Break LOCA) are selected as scenarios of simulation of sequence of SAs using MELCOR code. A small break of 1.35" in the cold leg is assumed for the base case of SBLOCA. For the SBO base case, the off-site power is assumed to be lost. For the TLOFW base case, main feed water (MFW) and AFW are considered to be unavailable. The simulation data of wall temperature of reactor vessel and lower header is available from the calculated results of the seven data points placed outside of the reactor for sequence of events that occur from different severe accident scenarios. Locations for the data points for temperature measurement are RX Vessel Upper Plenum 1 Point (TW(1,1) HS-TEMP.20021), RX Vessel Core Wall 3 Point (TW(2,1) HS-TEMP.20013), (TW(4,1) HS-TEMP.20009), (TW(7,1) HS-TEMP.20004)) and Bottom hemisphere 3 Point (TB(1,1) COR-TLH.601), (TB(4,1) COR-TLH.301), (TB(7,1) COR-TLH.101).

5. Identification of In-vessel Phenomena

The simulation data of temperature from 7 data points are labelled as HS-TEMP2002104, HS-TEMP.2001304, HS-TEMP.2000904, HS-TEMP.2000404, COR-TLH.601, COR-TLH.301, COR-TLH.101. The true temperature data is added

with random white Gaussian noise of standard deviation 0.1 to depict practical measurement conditions. To analyze the estimation results of IMM and KF we selected two data points of the reactor core information and COR-TLH.301 which is at bottom middle hemisphere of reactor vessel. The results for wall temperature distribution with IMM and KF for SA scenario, SBO corresponding to HS-TEMP.2000404 and COR-TLH.301 are shown in Figure 2 and Figure 3.

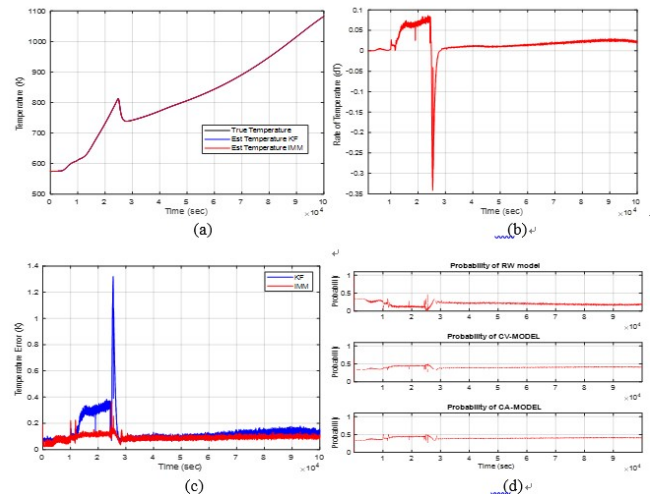


Figure 2. Results for wall temperature estimation in SBO scenario for point 4 (HS-TEMP.2000404) (a) estimated outer wall temperature using KF and IMM (b) estimated rate of temperature with IMM (c) temperature estimation error (d) model probabilities

Figure 2 shows the estimation result of wall temperature distribution and the rate of temperature for HS-TEMP.2000404. In Figure 2 (a), it can be noticed that the temperature starts to rise continuously after 3400 sec and at about 11711 sec the rate of temperature rise is more and a sudden increase of 190 K is observed in the next 13000sec and the temperature drops around 74 K and then again increases continuously to near about 1082 K in 99990sec. The dT plot in Figure 2(b), the slope of the curve gives us better idea about the temperature variation. The positive dT value suggest there is increase in wall temperature and negative value suggest there is decrease in wall temperature. Using T and dT plots of Figure 2 we can identify the sequence of SA events. The initial rise in temperature around 3400 sec can be identified as start of dry out condition and around 11711 sec as start of core relocation, that is melting of fuel, corium and around 24780 sec where temperature starts to drop it can be identified as start of reflooding and after 27820 sec the temperature increases again which can be identified as end of reflooding. Difference of the axial temperature between the top, middle and bottom position is not much in terms of the sequence of severe accident scenarios. But it can be identified that the axial temperature of top, middle and bottom position is rapidly increasing or decreasing at start of dry out condition and start of core relocation and start of reflooding. The temperature

estimation error is shown in Figure 2(c) where the wall temperature is estimated with good accuracy by IMM and KF. However, IMM has better estimation performance as compared to KF when the distribution changes abruptly and has nonlinear or linear behavior. The model probabilities for each model used in IMM with respect to time is shown in Figure 2(d).

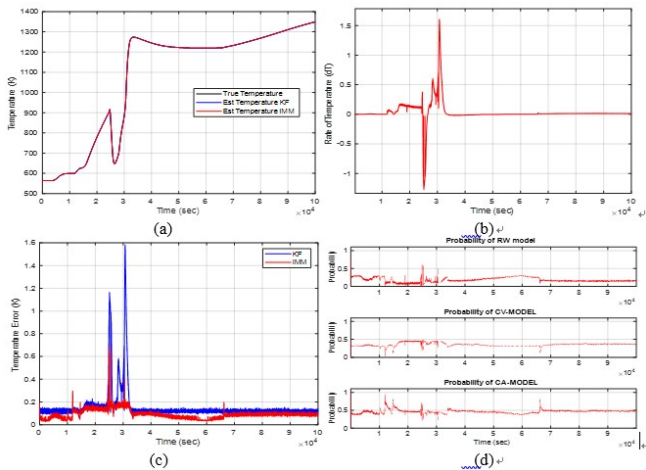


Figure 3. Results for wall temperature estimation in SBO scenario for point 6 (COR-TLH.301) (a) estimated outer wall temperature using KF and IMM (b) estimated rate of temperature with IMM (c) temperature estimation error (d) model probabilities

Figure 3 shows the estimation result of wall temperature distribution and the rate of temperature for bottom hemisphere data point COR-TLH.301. The estimation results for wall temperature distribution are shown in Figure 3(a) and the rate of temperature in Figure 3(b). There is temperature rise continuously after 3460 sec and then further after 11651 sec, temperature rises more rapidly as compared to reactor core area (HS-TEMP.2000404) the rise is about 300K in 12000 sec and then after 24580 sec, the temperature drops about 260 K until 26630 sec and then again there is enormous sudden rise of temperature near about 1273 K in very short period of time and then after that temperature drops to 1220 K and it is constant for a period of time and then again increases further up to 1350 K. The dT plot (Figure 3(b)) shows the rate of temperature where the slope and magnitude of curve are higher as compared to HS-TEMP.2000404. From T and dT plots in Figure 3, we can identify the region around 3460 sec as start of dry out condition and around time steps 11651 sec where dT slope shows positive spike and it can be identified as start of core relocation, at around time steps 24580 sec when the dT curve slope is negative it can be identified as start of reflooding and at 26630 sec when temperature start to rise sharply and dT is positive, it can be termed as end of reflooding and with very rapid rise in temperature with positive dT value and high magnitude around time 33250 sec it can be termed as reactor failure. The performance comparison of KF and IMM for temperature estimation is shown in Figure 3(c) as it is seen IMM has good estimation as

compared to KF especially when the temperature increases linearly or non-linearly. The model probabilities for each KF model used in IMM with respect to time are shown in Figure 3(d). Difference of the temperature between of top, middle and bottom hemisphere is not much in terms of the sequence of severe accident scenarios. But it can be identified that the temperature of top, middle and bottom hemisphere is rapidly increasing or decreasing at start of dry out condition and start of core relocation, start of cooling water injection and reflooding, and reactor failure.

Figure 4 shows the T and dT IMM estimation results for 7 data points for SBO scenario. In case of SBO, the bottom hemisphere of reactor vessel has large temperature fluctuation compared to reactor core area and Upper Plenum. As seen from the figure 4, the sequence of SA such as dry out, core relocation and cooling water injection, reflooding for the bottom hemisphere data points appear before as compared to the data points on reactor core and upper plenum, and moreover dT slope for bottom hemisphere has more magnitude that signifies the temperature change is more rapid. From figure 4, the wall temperature distribution of bottom hemisphere, we can see the very rapid temperature rise and dT slope shows positive spike and it can be identified that the real core relocation is to be starting more earlier as seen from the data point COR-TLH.101(yellow) in the figure 4 comparing with the data points HS-TEMP.2000404 on reactor core.

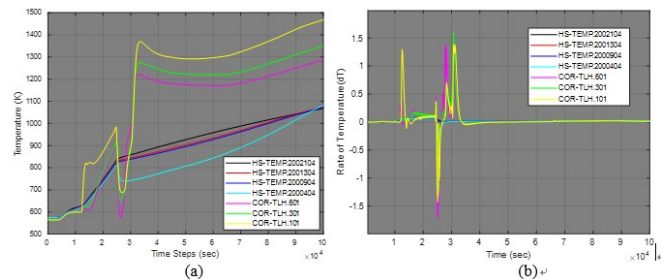


Figure 4. Results for wall temperature estimation for all seven data points in SBO scenario (a) estimated outer wall temperature using IMM at different locations of reactor (b) estimated rate of temperature

6. Conclusions

An algorithm based on IMM-FDD is developed for identification of in-vessel phenomena during severe accident. Identification is done from the estimated out-wall temperature measurement recorded outside of reactor vessel. Multiple models using random walk, constant velocity and constant acceleration are used to describe the evolution of transient temperature. Proposed IMM-FDD scheme is applied to the wall temperature containing various SA scenarios initiated by SBO, TLOFW, SBLOCA, MBLOCA and LBLOCA which are simulated using MELCOR code. It is found that the proposed IMM-FDD can estimate the wall temperature of core region with good accuracy and the rate of temperature can be used to identify the in-vessel phenomena during progression of SA. From the final estimates of wall temperature and rate of temperature, the sequence of in-vessel phenomena is classified

as core dry out, corium relocation, reflooding, and reactor failure. IMM has better estimation of wall temperature as compared to KF when the temperature distribution changes abruptly and has nonlinear or linear behavior.

Acknowledgement

This work was supported by the National Research Foundation of Korea (NRF) grant funded by the Korean government (MSIT: Ministry of Science and ICT) (No. 2017M2A8A4017932). This work was supported by the research grant of Jeju National University in 2020.

REFERENCES

- [1]. C.K. Lau, K. Ghosh, M.A. Hussain, C.C. Hassan, Fault diagnosis of Tennessee Eastman process with multi-scale PCA and ANFIS, *Chemom. Intell. Lab. Syst.*, 120, (2013), 1-14.
- [2]. I.S. Lee, J.T. Kim, J.W. Lee, D.Y. Lee, K.Y. Kim, Model-based fault detection and isolation method using ART2 neural network, *International journal of intelligent systems*, 18(2003), 1087-1100.
- [3]. X.R. Li, and Y. Zhang, Multiple model estimation with variable structure, *IEEE trans. Automatic. Control*, 41, (1996), 478-493
- [4]. B.S. Kim, U.Z. Ijaz, J.H. Kim, M.C. Kim, S. Kim, K.Y. Kim, Nonstationary phase boundary estimation in electrical impedance tomography based on the interacting multiple model scheme, *measurement Science and Technology*, 18, (2006), 62.
- [5]. M.J. Peng, H. Wang, S.S. Chen, G.L. Xia, Y.K. Liu, X. Yang, A. Ayodeji, An intelligent hybrid methodology of on-line system-level fault diagnosis for nuclear power plant, *Nuclear Engineering and Technology*, 50, (2018), 396-410
- [6]. Z. Zhang, J. Chen, Fault detection and diagnosis based on particle filters combined with interactive multiple-model estimation in dynamic process systems, *ISA transactions*, 85 (2019), 247-261.
- [7]. S.M. Kargar, K. Salahshoor, M.J. Yazdanpanah, Integrated nonlinear model predictive fault tolerant control and multiple model based fault detection and diagnosis, *Chem. Eng. Res. Des.*, 92, (2014), 340-349.
- [8]. B. Pourbabaee, N. Meskin, K. Khorasani, Multiple-model based sensor fault diagnosis using hybrid kalman filter approach for nonlinear gas turbine engines, In: 2013 American control conference (ACC), Washington, DC, USA, June 17-19, 2013.
- [9]. A. K. Khambampati, A. Rashid, U.Z. Ijaz, S. Kim, M. Soleimani, K.Y. Kim, Unscented Kalman filter approach to tracking a moving interfacial boundary in sedimentation processes using three-dimensional electrical impedance tomography, *Philosophical Transactions of the Royal Society A: Mathematical, Physical and Engineering Sciences*, 367, (2009), 3095-3120.